Electronic Supplementary Material (ESI) for Journal of Materials Chemistry A.

Electronic supplementary information

Ruthenium/Nitrogen-doped Carbon as an Electrocatalyst for Efficient Hydrogen Evolution in Alkaline Solution

Jian Zhang, Pan Liu, Gang Wang, Panpan Zhang, Xiaodong Zhuang, Mingwei Chen, I.M. Weidinger, Xinliang Feng*

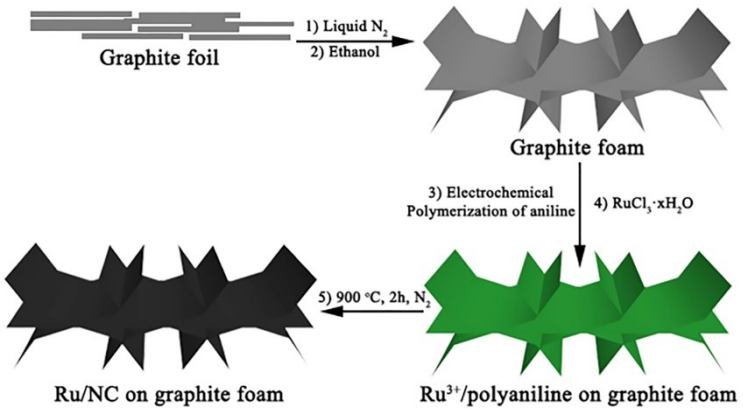

Fig. S1 Schematic illustration of Ru/NC preparation on the 3D graphite foam.

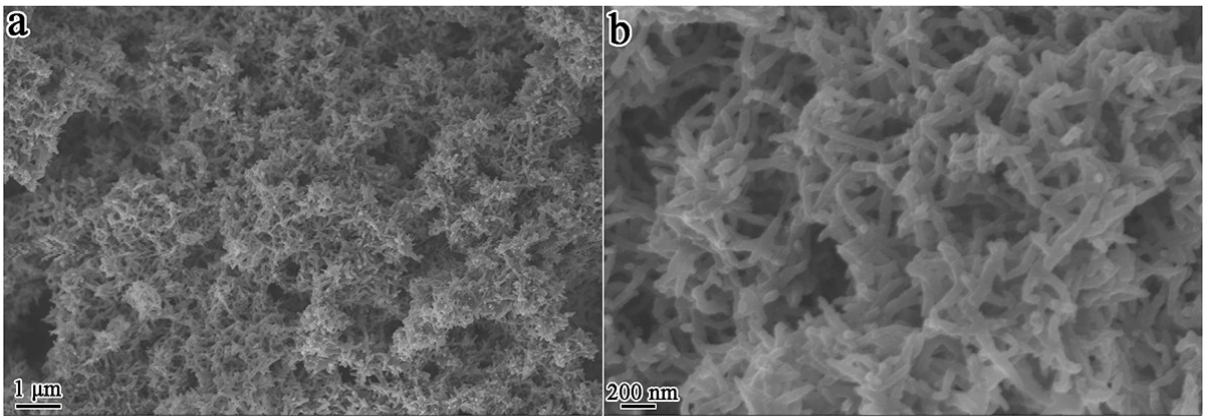

Fig. S2 SEM images of the polyaniline nanofibers on the 3D graphite foam.

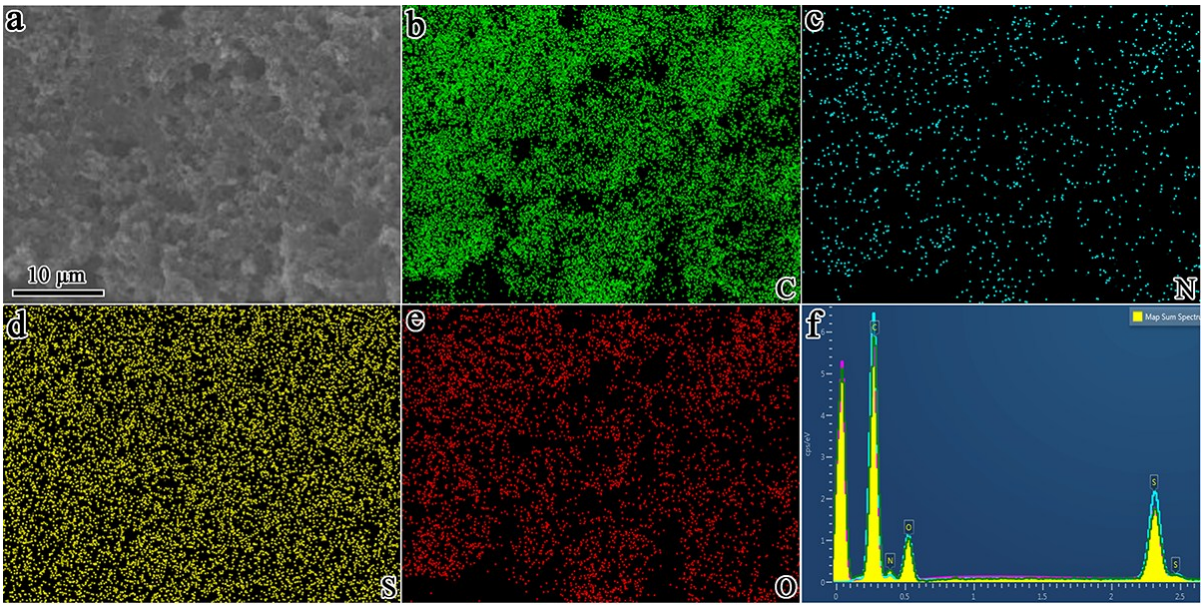

Fig. S3 a) SEM image and f) EDS analysis of polyaniline on the 3D graphite foam. The corresponding elemental mapping images of polyaniline on the 3D graphite foam: b) C, c) N, d) S and e) O.

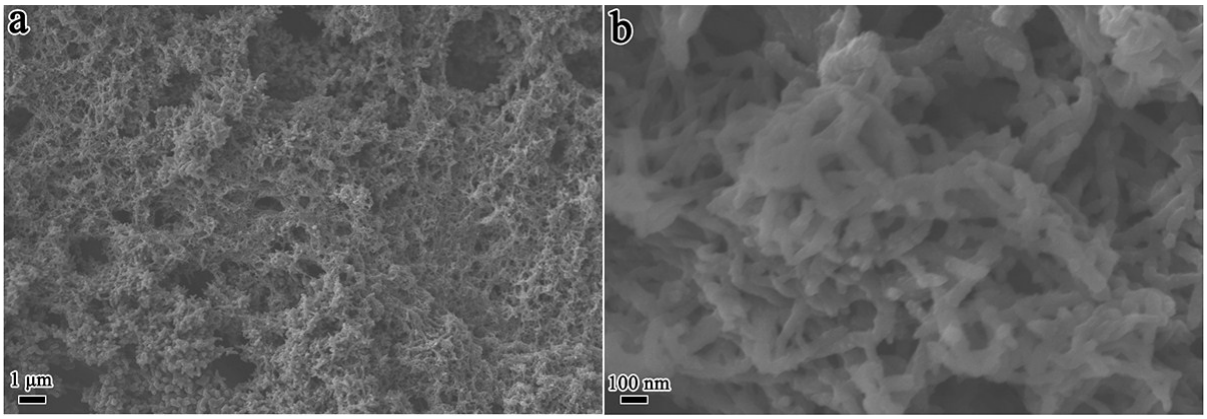

Fig. S4 a) SEM image of the Ru^{3+}/polyaniline complex on the 3D graphite foam.

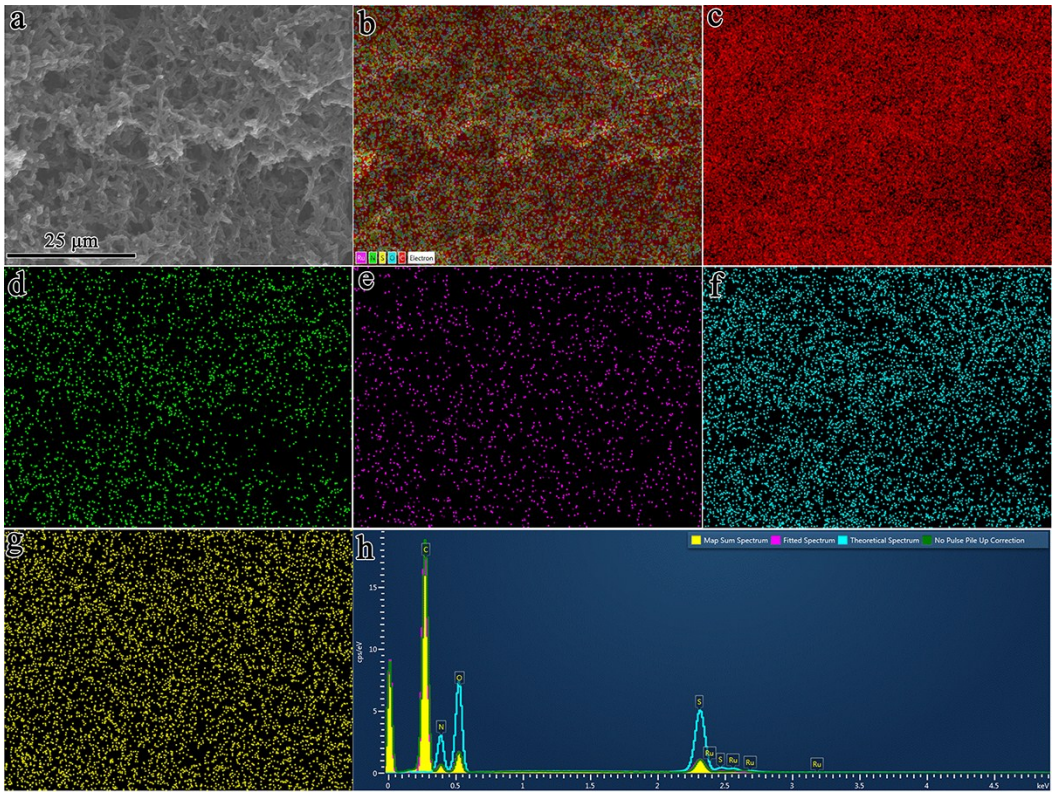

Fig. S5 a) SEM image and h) EDS analysis of the Ru^{3+}/polyaniline complex on the 3D graphite foam. The corresponding elemental mapping images of the Ru^{3+}/polyaniline complex on the 3D graphite foam: c) C, d) N, e) Ru, f) O and g) S.

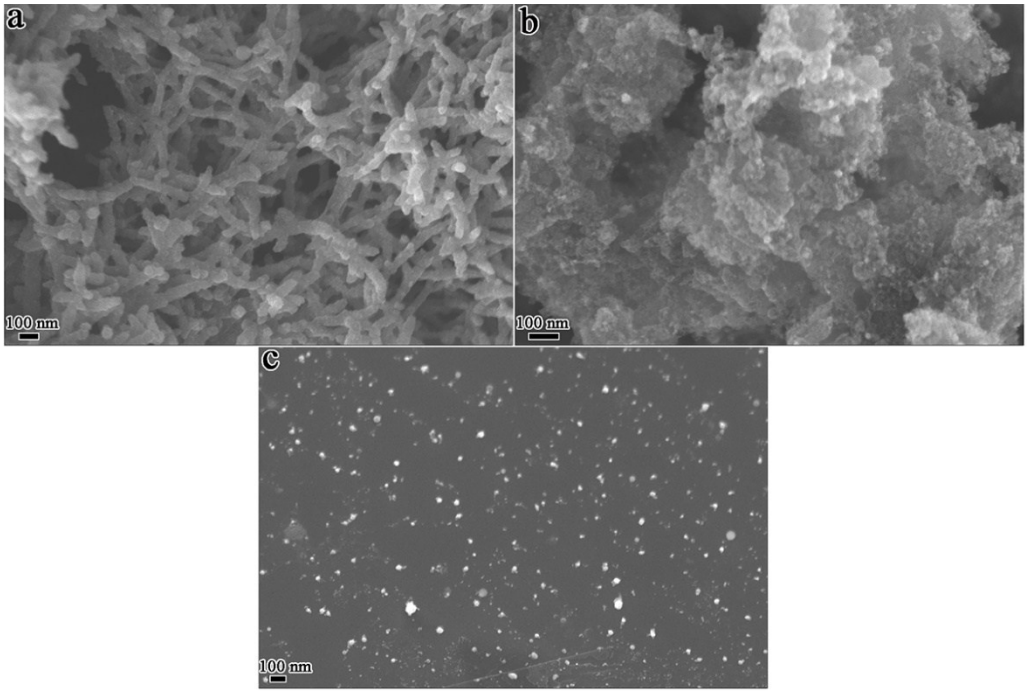

Fig. S6 SEM images of the samples synthesized at different temperatures: a) 800 °C, b) 900 °C and c) 1000 °C.

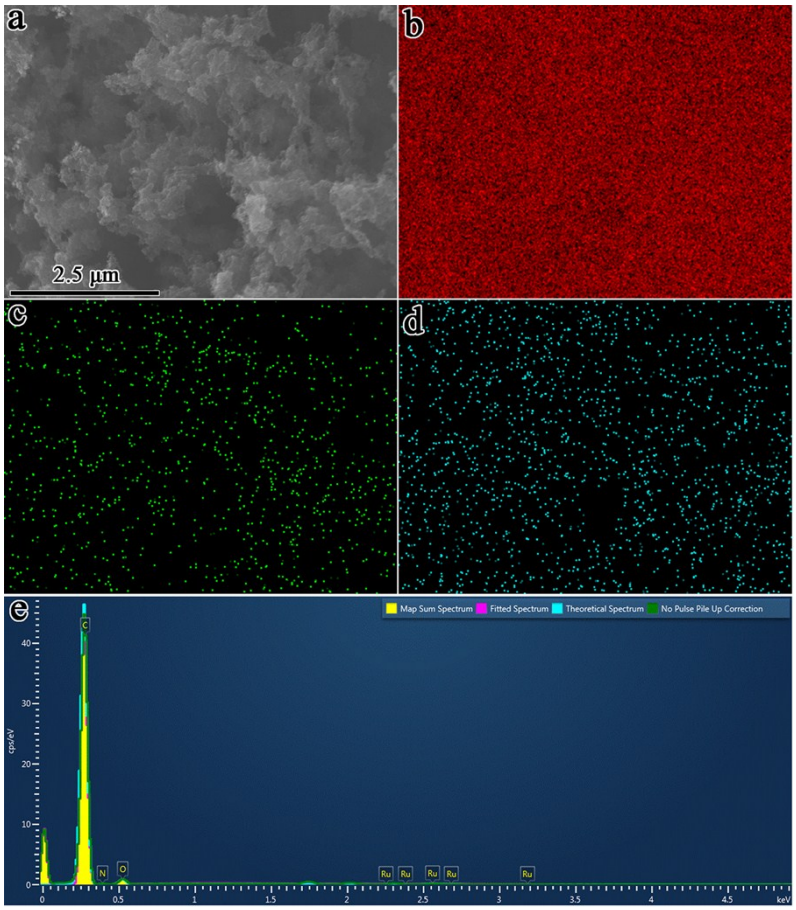

Fig. S7 a) SEM image and e) EDS analysis of the Ru/NC electrocatalyst on the 3D graphite foam. The corresponding elemental mapping images of the Ru/NC electrocatalyst on the 3D graphite foam: b) C, c) N, and d) Ru.

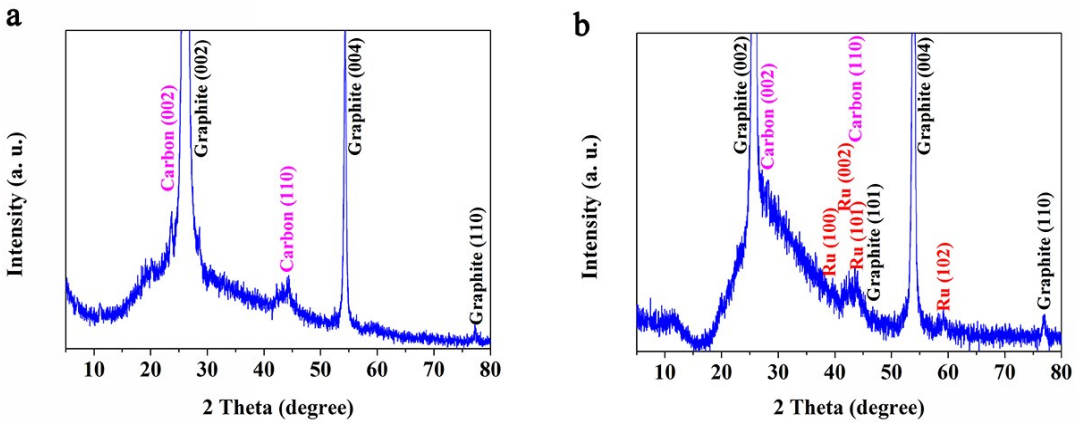

Fig. S8 XRD diffraction patterns of a) the NC and b) Ru/NC electrocatalysts. In Fig. S8B, the characteristic diffraction signals of the (100), (002), (101) and (102) facets of Ru appeared at 39.9°, 41.8°, 43.7° and 59.3°, respectively.

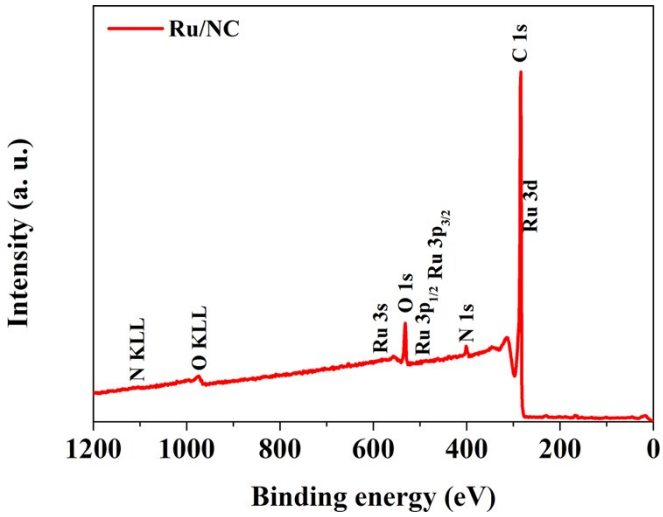

Fig. S9 XPS spectrum of the Ru/NC electrocatalyst.

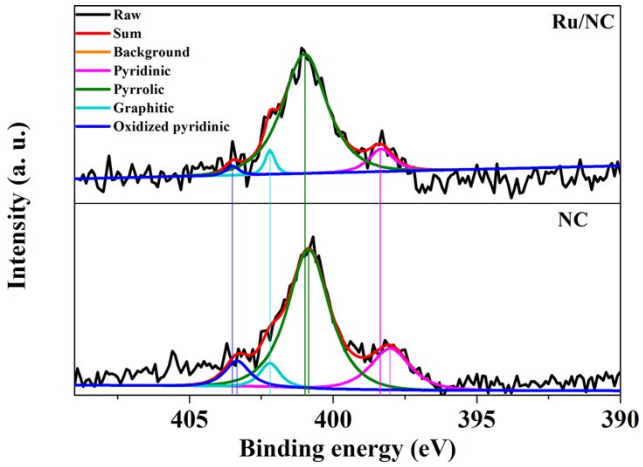

Fig. S10 High-resolution N 1s XPS patterns in the NC and the Ru/NC electrocatalysts.

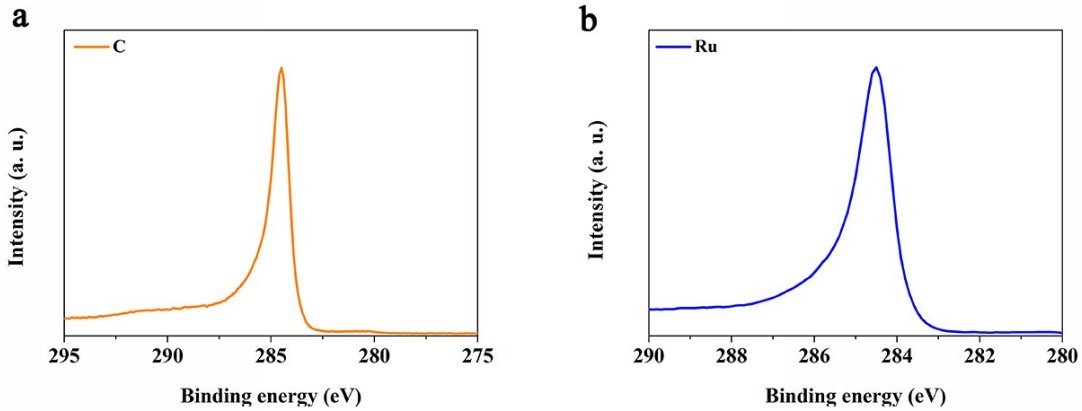

Fig. S11 XPS patterns of a) C 1s and b) Ru 3d in the Ru/NC electrocatalyst.

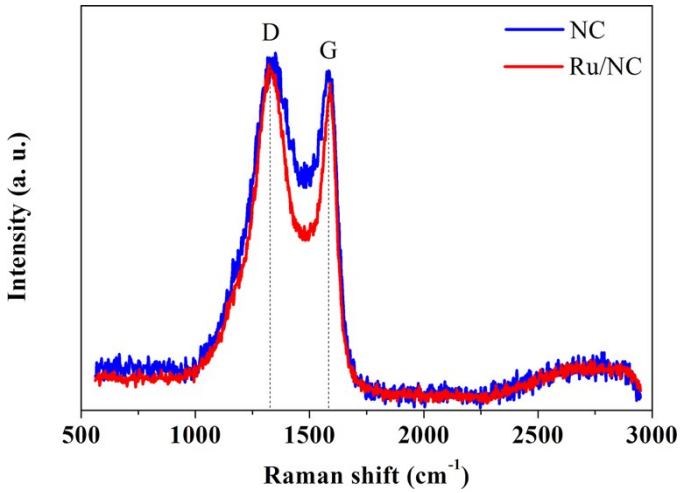

Fig. S12 Raman spectra of the NC and Ru/NC electrocatalysts. For the Ru/NC electrocatalyst, the D and G bands were observed at 1327.4 and 1583.8 cm^{-1}, respectively.

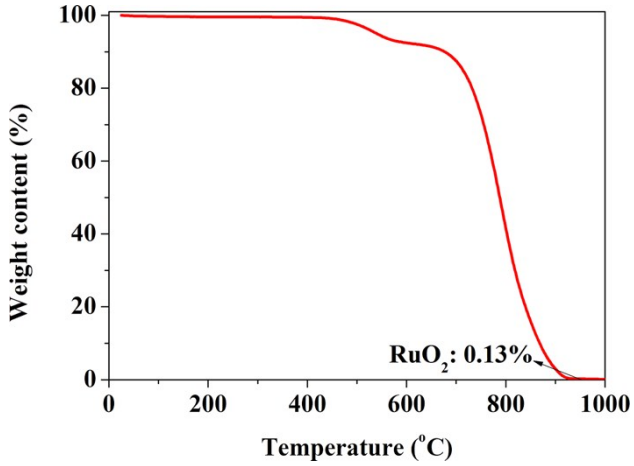

Fig. S13 TGA analysis of the Ru/NC electrocatalyst.

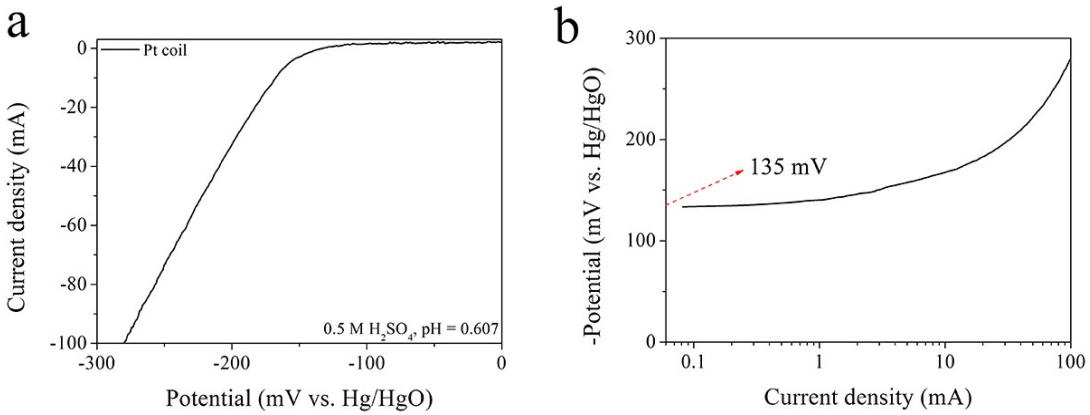

Fig. S14 (a) Polarization curve and (b) corresponding Tafel plot of a Pt coil in a H_2SO_4 aqueous solution (pH = 0.607). The standard potential (vs. RHE) of the Hg/HgO reference electrode was calibrated to be approximately 0.099 V.

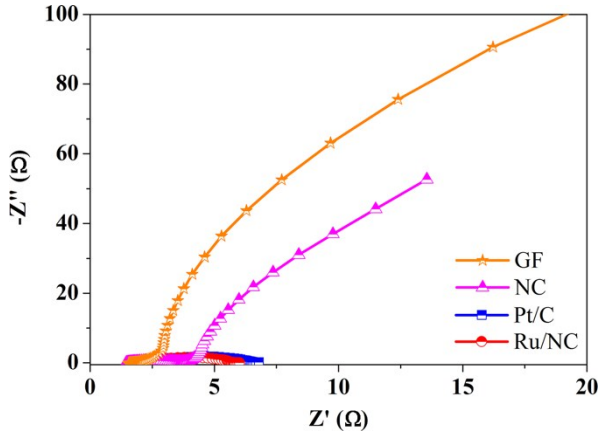

Fig. S15 Electrochemical impedance spectroscopy (EIS) analyses of the catalysts. The spectra were measured in an Ar-saturated 1 M KOH aqueous solution at -0.1 V vs. RHE with a 10 mV AC potential from 10 kHz to 0.01 Hz.

The recorded impedances are presented in the form of imaginary (Im) vs. real (Re) parts at various frequencies. It has been recognized that the high frequency intercept of the Re-axis represents the resistance of the electrodes. The width of the semicircle on the Re-axis corresponds to the charge-transfer resistance and indicates the overall kinetic effects. As indicated in Fig. S14, all of the electrocatalysts exhibited nearly the same intrinsic resistance (~1.32 ohm), whereas the charge-transfer resistance of the Ru/NC electrocatalyst was much lower than that of the GF and NC electrocatalysts, suggesting a faster HER kinetic process on the Ru/NC electrocatalyst.

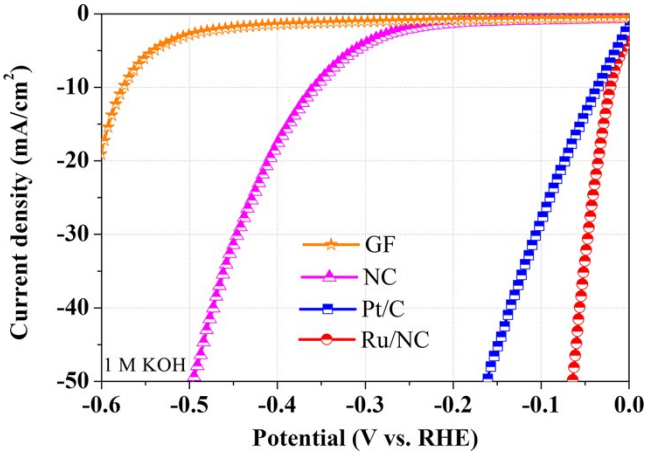

Fig. S16 Polarization curves of the GF, NC, commercial Pt/C and Ru/NC electrocatalysts.

Table S1 HER activities of the as-prepared Ru/NC electrocatalyst and other reported electrocatalysts.

Electrocatalysts	Onset overpotential (mV)	Overpotential (mV) at 10 mA/cm^2	Tafel slope (mV/decade)	TOF (s^{-1})	Electrolyte
Ru/NC (this work)	**0**	**21**	**31**	**4.55 (100 mV)**	**1 M KOH**
Pt/C	0	30	31	1.41 (100 mV)	1 M KOH
NiO/Ni heterostructures[1]	0	30	51	—	1 M KOH
Co-Mo-S_x chalcogels[2]	60	210 mV at 5 mA/cm^2	—	—	0.1 M KOH
	100	235 mV at 5 mA/cm^2	—	—	0.1 M $HClO_4$
MoP[3]	50	130	48	—	1 M KOH
Co@N-doped CNTs[4]	140	370	>69	—	1 M KOH
Pt nanowires/single layer $Ni(OH)_2$ nanosheets[5]	5	98 mV at 5 mA/cm^2	—	—	1 M KOH
MoC_x nano-octahedrons[6]	80	151	59	—	1 M KOH
	25	142	53	—	0.5 M H_2SO_4
Pt_3Ni_3 nanowires[7]	0	50	—	—	1 M KOH
Cr_2O_3/NiO/Ni hybrid[8]	0	30	—	—	1 M KOH
Co/Co_3O_4 core/shell nanosheets[9]	30	95	44	—	1 M KOH
c-$CoSe_2$[10]	80	200	85	—	1 M KOH
Mo_xC/Ni@N-doped carbon[11]	20	126	—	—	1 M KOH
MoB[12]	150	220	59	—	1 M KOH
Ni-Mo nanopowders[13]	20	90	—	—	1 M KOH
N,P-doped Mo_2C@carbon nanospheres[14]	0	50	71	3.71×10^{-3} (10 mV)	1 M KOH
WC nanocrystals/CNTs[15]	45	150	106	—	0.1 M KOH
$Zn_{0.3}Co_{2.7}S_4$ polyhedra[16]	40	100	48	—	0.1 M KOH
CoP nanowires/carbon cloth[17]	150	240	129	—	1 M KOH
Ni/CeO_2/CNTs[18]	30	91	—	—	1 M KOH
$Co(OH)_2$/PANI hybrid[19]	50	90	92	—	1 M KOH
Ru/C_3N_4/carbon	0	79	—	4.2 (100 mV)	0.1 M KOH
Ru/C_2N	0	17	38	0.75 (25 mV)	1 M KOH
RuCo alloy/carbon	0	28	31	—	1 M KOH
Pyrite-type CoPS nanowires[20]	15	48	48	—	0.5 M H_2SO_4
Strained MoS_2 nanosheets[21]	50	170	60	0.16	0.5 M H_2SO_4
W_2C nanoparticles[22]	50	123	45	—	0.5 M H_2SO_4
MoSSe/$NiSe_2$ foam[23]	20	69	42	—	0.5 M H_2SO_4
Pyrite-type CoPS/CNTs[24]	0	48	55	—	0.5 M H_2SO_4
Ni-doped carbon[25]	5	34	41	—	0.5 M H_2SO_4
Co-doped graphene[26]	30	180	82	0.22 (50 mV)	0.5 M H_2SO_4
Mo_2C/carbon/graphene[27]	0	34	34	—	0.5 M H_2SO_4
$WO_{2.9}$ powder[28]	10	70	50	8.0 (100 mV)	0.5 M H_2SO_4
WO_2/carbon nanowires[29]	10	58	46	—	0.5 M H_2SO_4

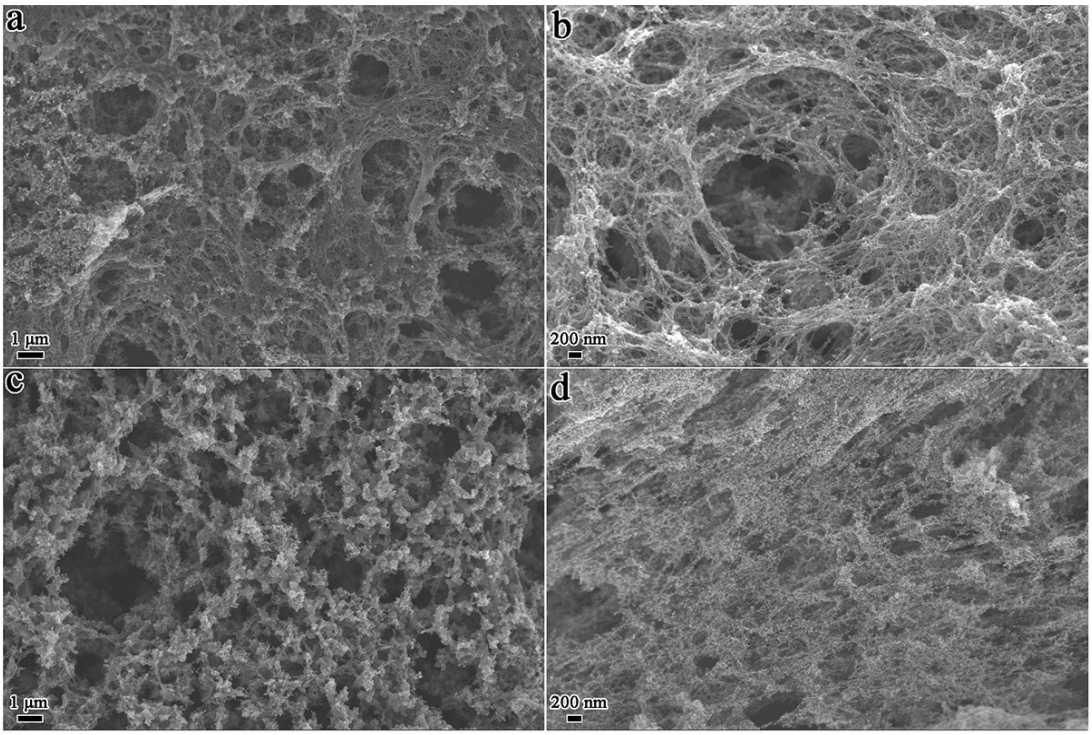

Fig. S17 SEM images of the Ru/NC electrocatalysts with different Ru contents: a) 0 μg, b) 6.5 μg, c) 13 μg and d) 26 μg.

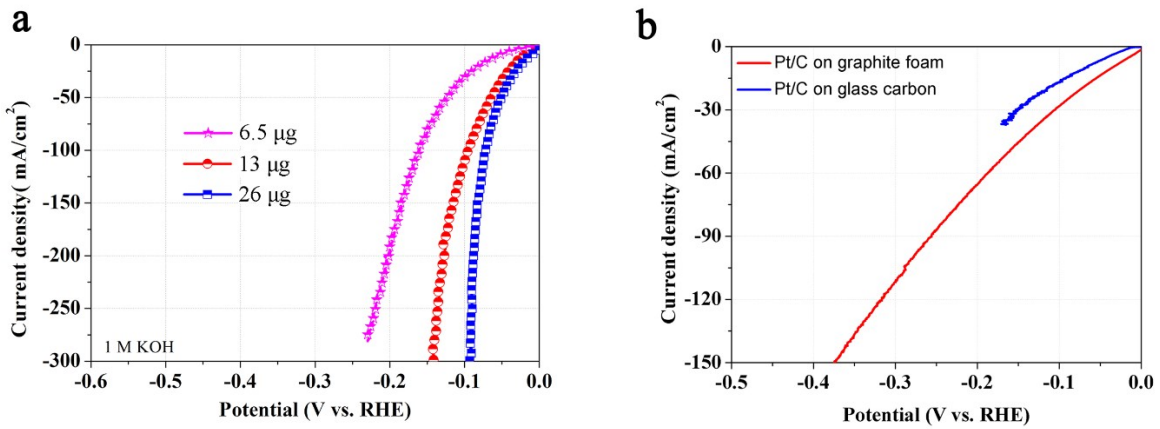

Fig. S18 a) Polarization curves of the Ru/NC electrocatalysts with different Ru loadings: 6.5 μg, 13 μg and 26 μg; b) polarization curves of the Pt/C deposited on the graphite foam or glass carbon electrode.

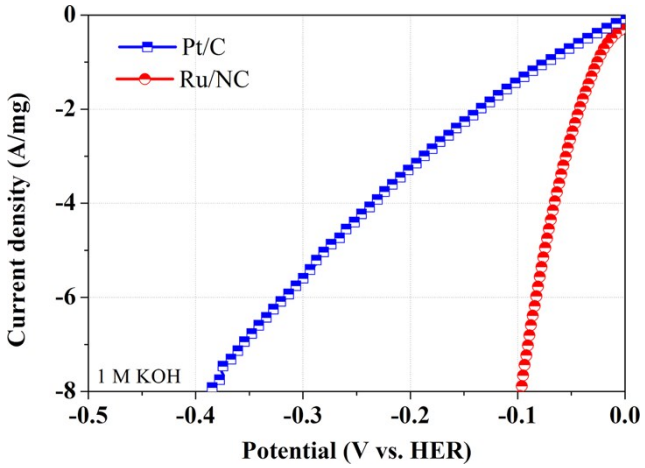

Fig. S19 Mass current density of the Ru/NC electrocatalyst and Pt catalyst.

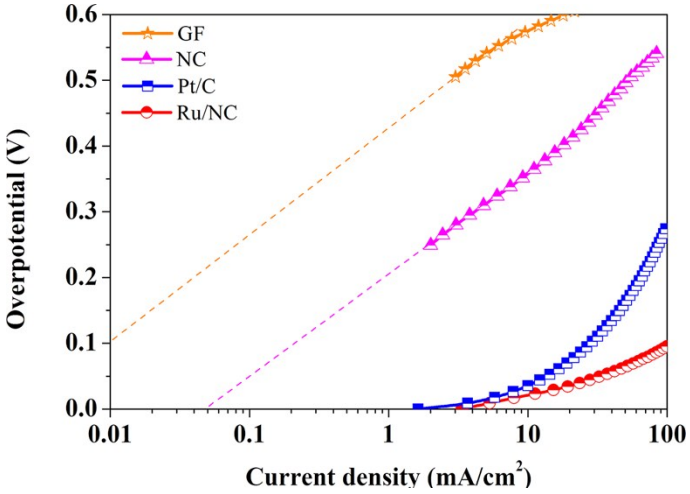

Fig. S20 Exchange current density of the GF, NC, commercial Pt/C and Ru/NC electrocatalysts.

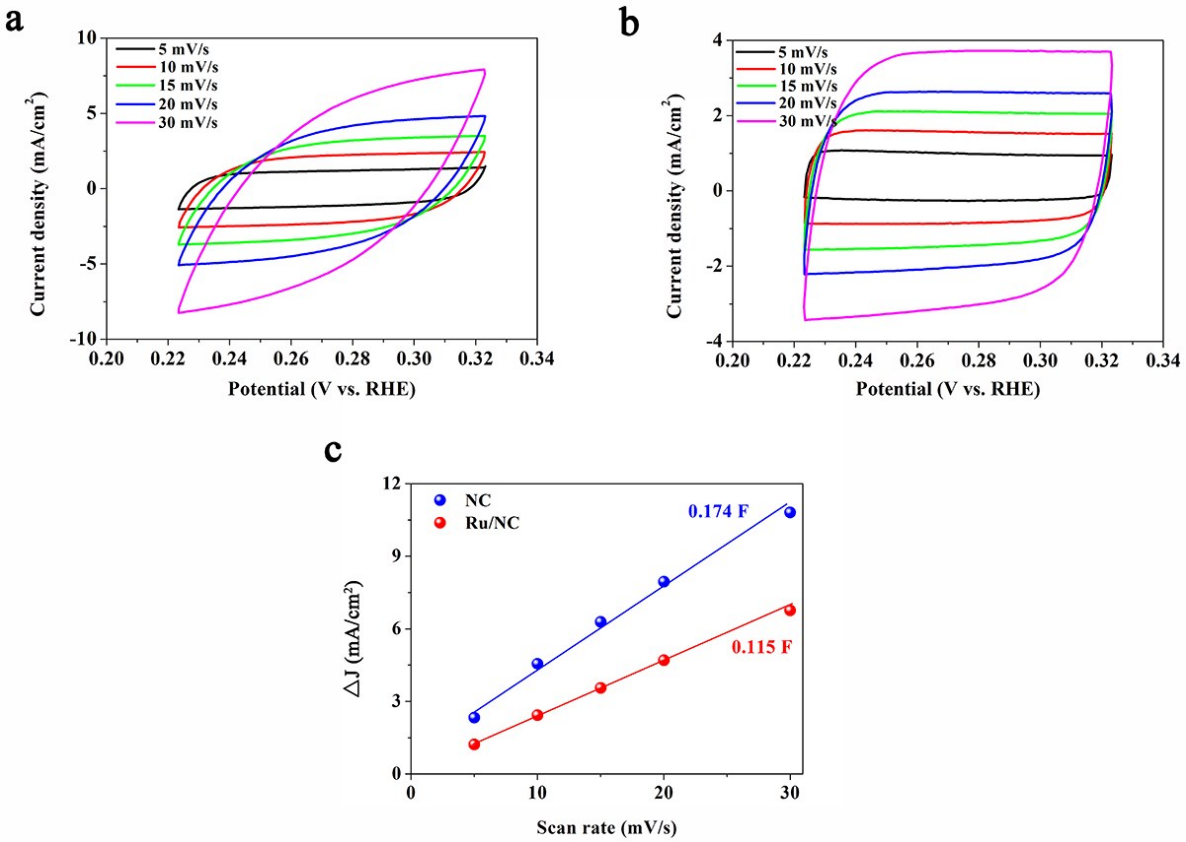

Fig. S21 The Cps of the NC and Ru/NC electrocatalysts were assessed using a series of cyclic voltammetry (CV) cycles at different scan rates. Cyclic voltammograms in the region 0.223 to 0.323 V (vs. RHE) were recorded at different scan rates: a) the NC electrocatalyst and b) the Ru/NC electrocatalyst. c) The difference in the current densities (∆J = Ja - Jc) at 0.273 V (vs. RHE) plotted against the scan rate and fit to a linear regression; Cp is 1/2 of the slope.

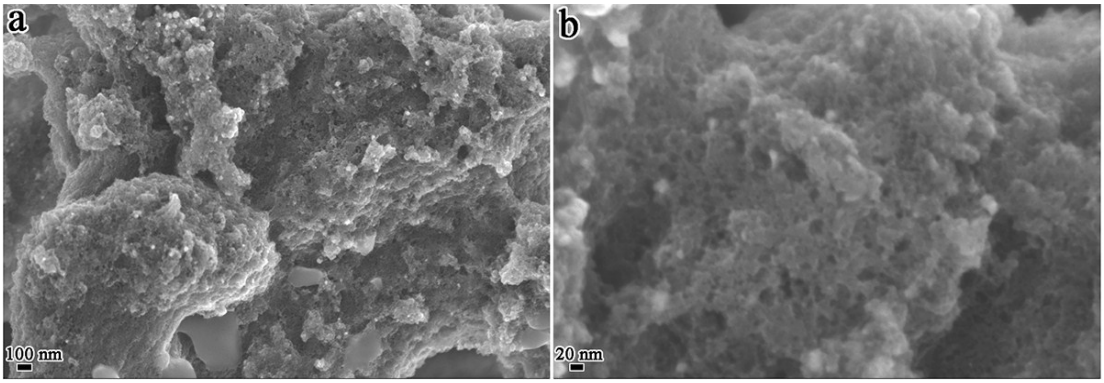

Fig. S22 SEM images of the Ru/NC electrocatalyst after the long-term HER stability test.

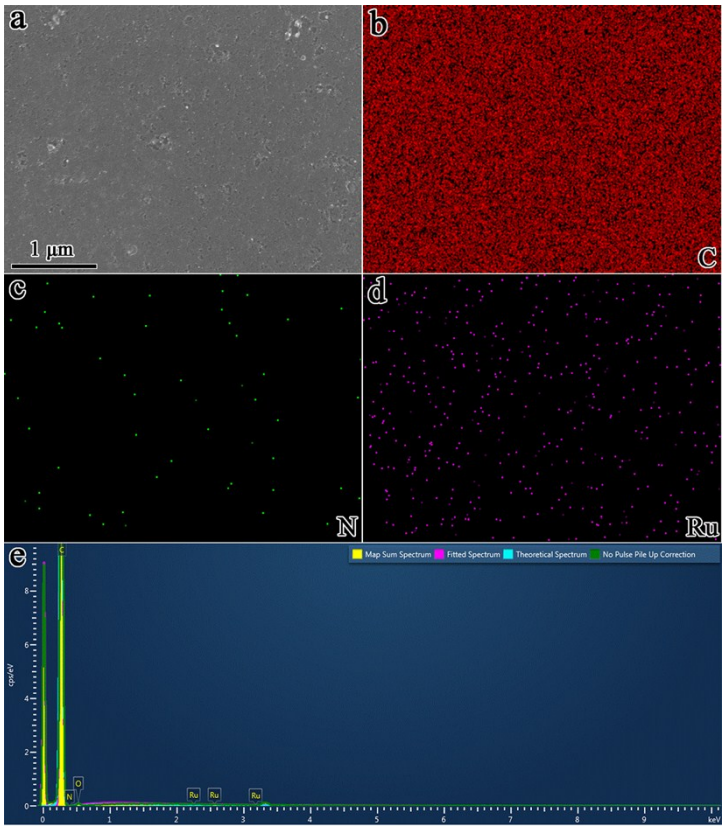

Fig. S23 a) SEM image and e) EDS analysis of the Ru/NC electrocatalyst after the long-term HER stability test. The corresponding elemental mapping images of the Ru/NC electrocatalyst: b) C, c) N, and d) Ru.

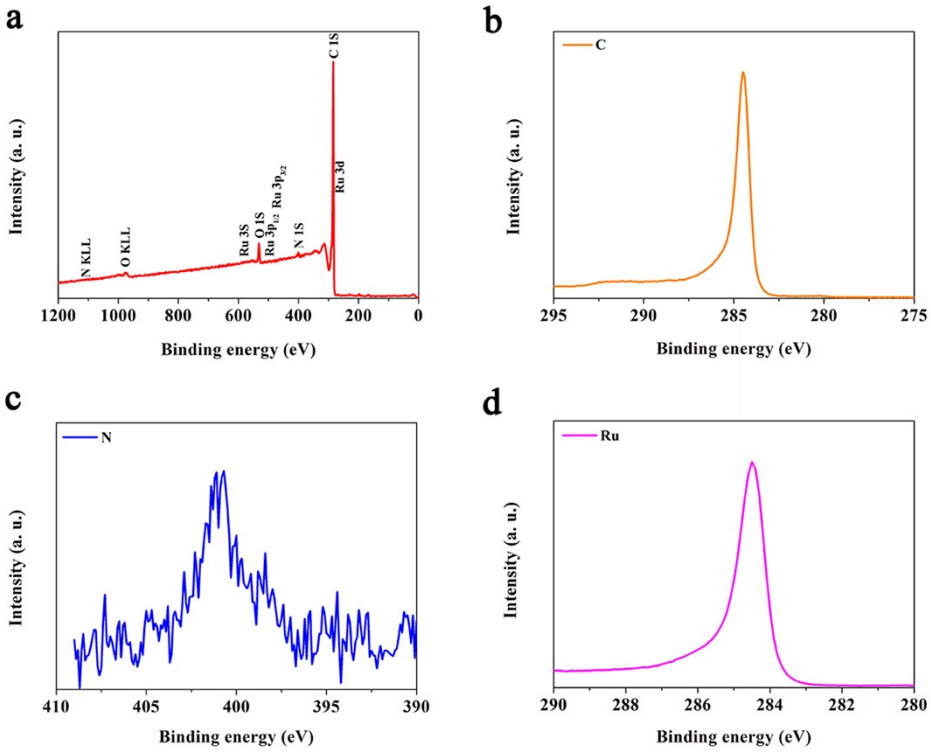

Fig. S24 a) XPS spectrum of the Ru/NC electrocatalyst after the long-term HER stability test. The corresponding high-resolution XPS patterns of the Ru/NC electrocatalyst after the long-term HER stability test: b) C 1s, c) N 1s, and d) Ru 3d.

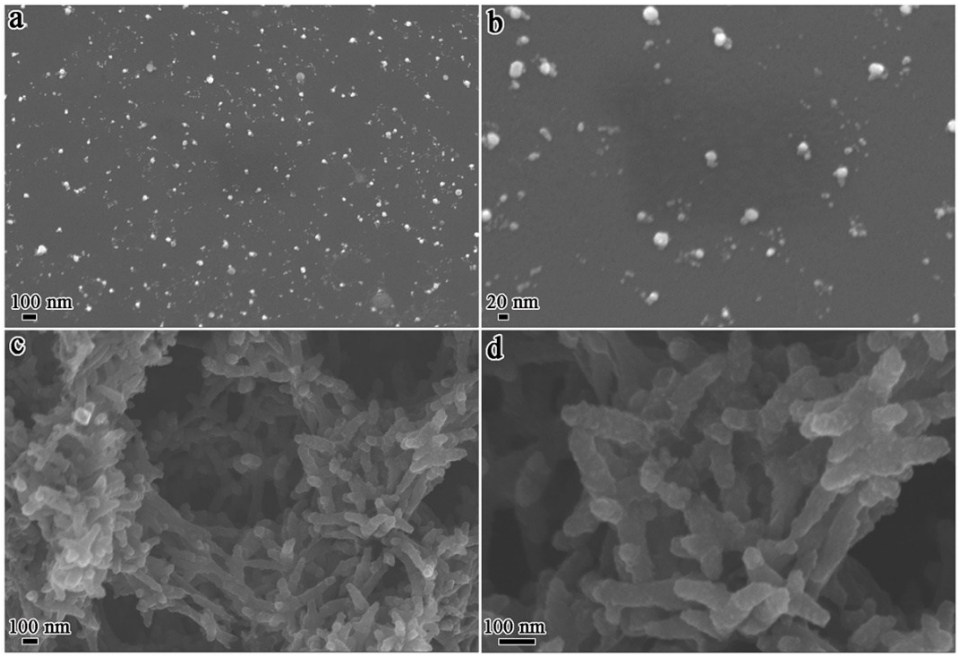

Fig. S25 SEM images of a and b) the Ru NPs and c and d) Ru NPs/NC on the GF.

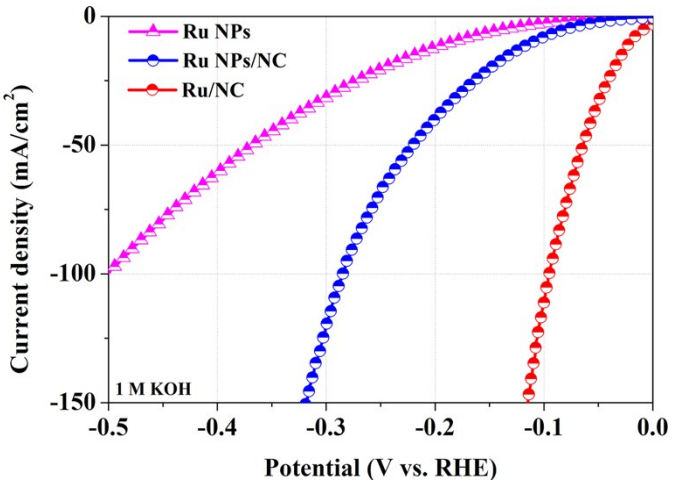

Fig. S26 Polarization curves of the Ru NPs, Ru NPs/NC and Ru/NC electrocatalysts in a 1 M KOH aqueous solution.

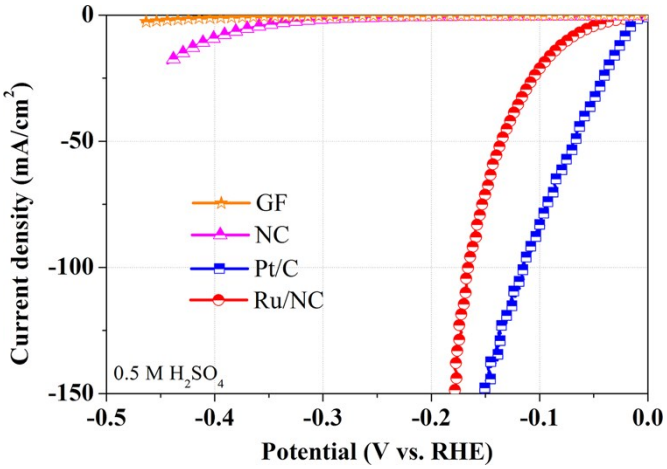

Fig. S27 Polarization curves of the GF, NC, commercial Pt/C and Ru/NC electrocatalysts in a 0.5 M H_2SO_4 aqueous solution.

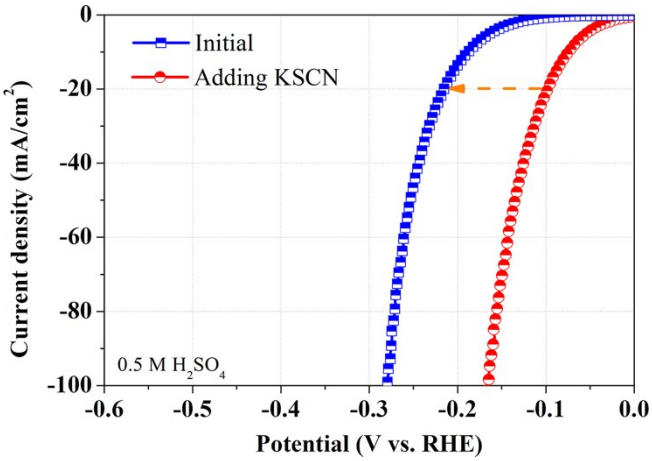

Fig. S28 HER polarization curves of the Ru/NC electrocatalyst with and without 10 mM KSCN in a 0.5 M H_2SO_4 aqueous solution.

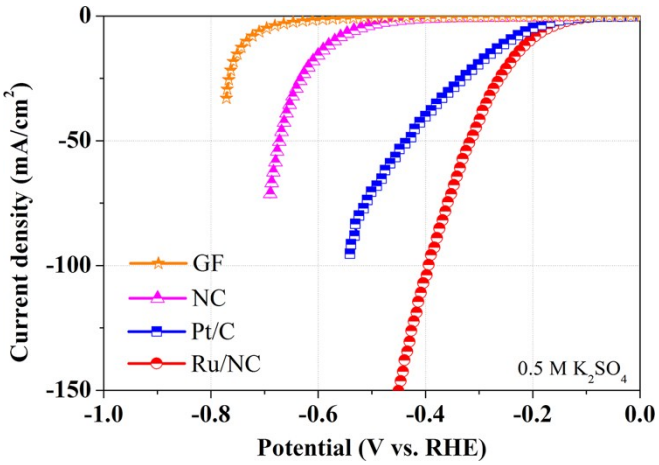

Fig. S29. Polarization curves of the GF, NC, commercial Pt/C and Ru/NC electrocatalyst in a 0.5 M K_2SO_4 aqueous solution.

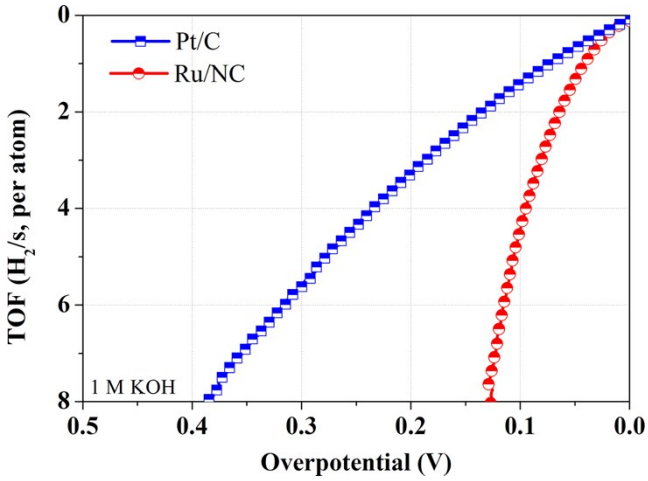

Fig. S30 TOF (per metal atom) plots for the Ru/NC electrocatalyst and the Pt catalyst.

Reference

[1] M. Gong, W. Zhou, M.-C. Tsai, J. Zhou, M. Guan, M.-C. Lin, B. Zhang, Y. Hu, D.-Y. Wang, J. Yang, Nat. Commun., 5 (2014) 4695-4700.

[2] J. Staszak-Jirkovsky, C. D. Malliakas, P. P. Lopes, N. Danilovic, S. S. Kota, K.-C. Chang, B. Genorio, D. Strmcnik, V. R. Stamenkovic, M. G. Kanatzidis, Nat. Mater., 15 (2016) 197-203.

[3] P. Xiao, M. A. Sk, L. Thia, X. Ge, R. J. Lim, J.-Y. Wang, K. H. Lim, X. Wang, Energy Environ. Sci., 7 (2014) 2624-2629.

[4] X. Zou, X. Huang, A. Goswami, R. Silva, B. R. Sathe, E. Mikmeková, T. Asefa, Angew. Chem.-Int. Edit., 126 (2014) 4461-4465.

[5] H. Yin, S. Zhao, K. Zhao, A. Muqsit, H. Tang, L. Chang, H. Zhao, Y. Gao, Z. Tang, Nat. Commun., 6 (2015) 6430-6437.

[6] H. B. Wu, B. Y. Xia, L. Yu, X.-Y. Yu, X. W. D. Lou, Nat. Commun., 6 (2015) 6512-6519.

[7] P. Wang, K. Jiang, G. Wang, J. Yao, X. Huang, Angew. Chem.-Int. Edit., 128 (2016) 13051-13055.

[8] M. Gong, W. Zhou, M. J. Kenney, R. Kapusta, S. Cowley, Y. Wu, B. Lu, M. C. Lin, D. Y. Wang, J. Yang, Angew. Chem.-Int. Edit., 127 (2015) 12157-12161.

[9] X. Yan, L. Tian, M. He, X. Chen, Nano Lett., 15 (2015) 6015-6021.

[10] P. Chen, K. Xu, S. Tao, T. Zhou, Y. Tong, H. Ding, L. Zhang, W. Chu, C. Wu, Y. Xie, Adv. Mater., 28 (2016) 7527-7532.

[11] S. Wang, J. Wang, M. Zhu, X. Bao, B. Xiao, D. Su, H. Li, Y. Wang, J. Am. Chem. Soc.,

137 (2015) 15753-15759.

[12] H. Vrubel, X. Hu, Angew. Chem.-Int. Edit., 124 (2012) 12875-12878.

[13] J. R. McKone, B. F. Sadtler, C. A. Werlang, N. S. Lewis, H. B. Gray, ACS Catal., 3 (2013) 166-169.

[14] Y.-Y. Chen, Y. Zhang, W.-J. Jiang, X. Zhang, Z. Dai, L.-J. Wan, J.-S. Hu, ACS Nano, 10 (2016) 8851-8860.

[15] X. Fan, H. Zhou, X. Guo, ACS Nano, 9 (2015) 5125-5134.

[16] Z.-F. Huang, J. Song, K. Li, M. Tahir, Y.-T. Wang, L. Pan, L. Wang, X. Zhang, J.-J. Zou, J. Am. Chem. Soc., 138 (2016) 1359-1365.

[17] J. Tian, Q. Liu, A. M. Asiri, X. Sun, J. Am. Chem. Soc., 136 (2014) 7587-7590.

[18] Z. Weng, W. Liu, L.-C. Yin, R. Fang, M. Li, E. I. Altman, Q. Fan, F. Li, H.-M. Cheng, H. Wang, Nano Lett., 15 (2015) 7704-7710.

[19] J. X. Feng, L. X. Ding, S. H. Ye, X. J. He, H. Xu, Y. X. Tong, G. R. Li, Adv. Mater., 27 (2015) 7051-7057.

[20] M. Cabán-Acevedo, M. L. Stone, J. Schmidt, J. G. Thomas, Q. Ding, H.-C. Chang, M.-L. Tsai, J.-H. He, S. Jin, Nat. Mater., 14 (2015) 1245-1251.

[21] H. Li, C. Tsai, A. L. Koh, L. Cai, A. W. Contryman, A. H. Fragapane, J. Zhao, H. S. Han, H. C. Manoharan, F. Abild-Pedersen, Nat. Mater., 15 (2016) 48-53.

[22] Q. Gong, Y. Wang, Q. Hu, J. Zhou, R. Feng, P. N. Duchesne, P. Zhang, F. Chen, N. Han, Y. Li, Nat. Commun., 7 (2016) 13216-13223.

[23] H. Zhou, F. Yu, Y. Huang, J. Sun, Z. Zhu, R. J. Nielsen, R. He, J. Bao, W. A. Goddard III, S. Chen, Nat. Commun., 7 (2016) 12765-12771.

[24] W. Liu, E. Hu, H. Jiang, Y. Xiang, Z. Weng, M. Li, Q. Fan, X. Yu, E. I. Altman, H. Wang, Nat. Commun., 7 (2016) 10771-10779.

[25] L. Fan, P. F. Liu, X. Yan, L. Gu, Z. Z. Yang, H. G. Yang, S. Qiu, X. Yao, Nat. Commun., 7 (2016) 10667-10673.

[26] H. Fei, J. Dong, M. J. Arellano-Jiménez, G. Ye, N. D. Kim, E. L. Samuel, Z. Peng, Z. Zhu, F. Qin, J. Bao, Nat. Commun., 6 (2015) 8668-8675.

[27] J.-S. Li, Y. Wang, C.-H. Liu, S.-L. Li, Y.-G. Wang, L.-Z. Dong, Z.-H. Dai, Y.-F. Li, Y.-Q. Lan, Nat. Commun., 7 (2016) 11204-11211.

[28] Y. H. Li, P. F. Liu, L. F. Pan, H. F. Wang, Z. Z. Yang, L. R. Zheng, P. Hu, H. J. Zhao, L. Gu, H. G. Yang, Nat. Commun., 6 (2015) 8064-8070.

[29] R. Wu, J. Zhang, Y. Shi, D. Liu, B. Zhang, J. Am. Chem. Soc., 137 (2015) 6983-6986.